

ORIGINAL RESEARCH ARTICLE

Hybrid log-sigmoid neural network with metaheuristic optimization for an $SEIIR$ diabetes mellitus model

Rashid Nawaz¹ , Saba Kainat^{2*} , and Muhammad Shoaib³ 

¹Department of Mathematics and Statistics, Faculty of Science, Universiti Putra Malaysia, Serdang, Selangor, Malaysia

²Department of Physics, University of Bologna, Bologna, Italy

³AI Center, Yuan Ze University, Taoyuan, Taiwan

Abstract

Diabetes mellitus is a complex metabolic disorder with diverse complications, which motivates the use of advanced computational intelligence methods for modeling its nonlinear dynamics. The goal of the current research is to obtain numerical solutions to a diabetes mellitus model by employing log-sigmoid neural networks together with both local and global search strategies. For this model, the genetic algorithm (GA) serves as a global search method, while the sequential quadratic programming approach is employed as a local optimizer. In this study, the problem is addressed using a hybrid solution strategy, introducing a new aspect to the existing research on diabetes mellitus modeling. The proposed model comprises five groups: susceptible, exposed, infected without treatment, infected with treatment, and recovered individuals. To compare the reliability, precision, and consistency of the proposed technique, the log-sigmoid neural network optimized through GA and sequential quadratic programming is compared with the Adam numerical solver. An absolute error within very small ranges is achieved, demonstrating the solver's proficiency. In addition, 100 independent trials and a network of 5 neurons were employed to test the validity of the proposed stochastic approach, together with statistical measures including root mean squared error, Theil's inequality coefficients, and mean absolute deviation.

Keywords: Diabetes mellitus model; Log-sigmoid neural networks; Genetic algorithm; Sequential quadratic programming

*Corresponding author:

Saba Kainat
(saba.kainat2@unibo.it)

Citation: Nawaz R, Kainat S, Shoaib M. Hybrid log-sigmoid neural network with metaheuristic optimization for an $SEIIR$ diabetes mellitus model. *Artif Intell Health*. 2026;3(2):025400081. doi: 10.36922/AIH025400081

Received: September 29, 2025

Revised: October 16, 2025

Accepted: October 28, 2025

Published online: December 31, 2025

Copyright: © 2025 Author(s). This is an Open-Access article distributed under the terms of the Creative Commons Attribution License, permitting distribution, and reproduction in any medium, provided the original work is properly cited.

Publisher's Note: AccScience Publishing remains neutral with regard to jurisdictional claims in published maps and institutional affiliations.

1. Introduction

Neural networks are representations of the neural circuits and neuronal activity found in the brain that may simulate many biological systems and processes. The genetic algorithm (GA) was developed based on the genetic evolutionary process observed in nature. It is a conventional intelligent biomechanical algorithm with considerable global optimization abilities. GA optimization may be used to train the neural network efficiently, and the training algorithm can purposefully ignore certain outputs depending on the requirements. Once the search problem has been encoded in a chromosomal fashion and a fitness metric

has been selected to differentiate between excellent and poor solutions, the GA can proceed through the following stages to evolve optimal solutions: initialization, evaluation, selection, recombination, mutation, and replacement.¹ The GA is used in various fields to determine the most effective way to solve problems, including fuzzy problems,² agriculture,³ medical treatments,⁴ the routing-allocation model,⁵ and numerous others.⁶⁻⁸

In recent years, sequential quadratic programming (SQP) techniques for extensive nonlinear optimization have made significant progress. The network's weights can be learned using the SQP algorithm, a powerful and precise solver for convergent optimization problems. In this study, the design variable output from the GA serves as the foundation for the SQP approach's initial estimation. Studies related to SQP are well-known in the scientific literature for solving various problems.⁹⁻¹¹

According to Wang,¹² combining a GA with a common local search method, such as SQP, can lead to a successful and consistent solution of a problem. SQP requires fewer calls for target and functional restrictions than GA. It may, however, become distorted and stuck in local optima, as the search method relies on gradient data. In contrast, the GA adopts a wider approach and has a higher probability of finding a global optimum throughout the whole process. The results are then utilized in SQP and local searching.¹³⁻¹⁵

Furthermore, the log-sigmoid neural network optimized through the GA and SQP (LSNN-GASQP) framework seamlessly combines the adaptive learning capability of neural networks, the global search efficiency of evolutionary algorithms, and the fast convergence of local optimization techniques. This hybrid methodology serves as a powerful numerical strategy for tackling nonlinear, stiff, and chaotic systems in applied mathematics, with significant applications in infectious disease modeling, fractional-order systems, and bio-mathematical dynamics. This research explores diabetic mellitus (DM) using LSNN-GASQP. DM, a metabolic disorder, is caused by impairments in insulin secretion, action, or both. The significance of gastrointestinal symptoms as a major contributor to disease burden in DM is well known.¹⁶ People with diabetes experience gastrointestinal symptoms, such as bloating, nausea, diarrhea, constipation, and epigastric fullness, more frequently. Depression is a common complication in diabetic patients, and if left unidentified and untreated, it can adversely influence the disease.¹⁷ Insulin resistance is closely related to obesity, and when combined with relative insulin insufficiency, it can lead to the development of type 2 DM.¹⁸ Dry eye disease is a lesser-known consequence of DM, although it is reported to occur in 54.3% of cases in individuals with the condition.¹⁹

Numerous ocular symptoms are also associated with DM, including micro- and macrovascular diseases.²⁰

Diabetic kidney disease, which eventually emerges in approximately 50% of individuals with type 2 DM, is the main factor contributing to the increased mortality risk in diabetic patients.²¹ To establish and sustain long-term good metabolic control in DM patients, a combination of lifestyle changes and prescribed medications is necessary. Achieving near-normal glycated hemoglobin levels significantly decreases the risk of macrovascular and microvascular issues. There are currently several oral and injectable medicines available for the treatment of type 2 DM.²² Diabetic patients have been shown to benefit from both aerobic and resistance-based exercises, which increase glucose uptake and decrease insulin resistance. Over the years, DM mechanics have been the focus of intense research by several researchers.²³⁻²⁵

Recently, the scientific community has employed stochastic computing frameworks and advanced neural network architectures to address intricate nonlinear problems in diverse scientific and technical fields. For example, Sabir *et al.*²⁶ devised a neuro-swarming methodology to address the Emden–Fowler nonlinear model. Ali *et al.*²⁷ created an intelligent solver utilizing evolutionary cubic splines for the nonlinear Painlevé-I transcendent problem. Umar *et al.*²⁸ proposed an intelligent computational method for modeling the nonlinear dynamics of human immunodeficiency virus infection. Cui *et al.*²⁹ analyzed the bidirectional associative memory neural network and introduced a scheme to delay bifurcation. Ilyas *et al.*³⁰ developed a wavelet neural network for the Falkner–Skan system in fluid dynamics. Raja *et al.*³¹ linked an artificial neural network with SQP to investigate Troesch's problem, whereas Ahmad *et al.*³² developed a comprehensive neuro-evolutionary solver for the nonlinear corneal shape model.

This study aims to tackle the DM nonlinear model using LSNN-GASQP-based stochastic numerical computation, taking into account the significant reported results. The advanced intelligent computer method offers several distinct advantages over current studies on DM. LSNN-GASQP surpasses prior models in anticipated efficacy and precision, providing more reliable insights into the processes of DM transmission. Our study leverages cutting-edge breakthroughs in computational intelligence, which significantly impact disease modeling and control, offering a more nuanced understanding of this complex epidemiological system.

In this study, we evaluated the solution of the system of nonlinear DM model³³ using the capabilities of LSNN and both local GA and global SQP optimum approaches. The

following is a list of the key characteristics of the proposed LNNASQP:

- (i) A novel use of LSNN is proposed to investigate the DM model, utilizing the combination of GA and SQP as global and local search techniques
- (ii) The Adam numerical methodology with absolute error analysis is used to compare the sustainability, reliability, and effectiveness of the proposed paradigm
- (iii) By applying the equations from the nonlinear DM model to an activation function, the mean squared error formulation of the fitness-based function is transformed into LSNN-GASQP
- (iv) Statistical analyses, including root mean squared error, Theil's inequality coefficients, and mean absolute deviation, are used to validate the accuracy and reliability of the LSNN-GASQP.

With the mathematical model described by Faisal *et al.*,³⁴ which divides the human population into five groups, such as the susceptible group $S(t)$, the exposed group $E(t)$, the infected group without treatment $I(t)$, the infected group with treatment $I_T(t)$, and recovered individuals $R(t)$. We explored the dynamics of a DM model in the following way, as shown in Equation (1):

$$\begin{cases} S'(t) = \nu - (\zeta + \psi E(t) + \omega)S(t), \\ E'(t) = (\psi E(t) + \omega)S(t) - (\zeta + 1)E(t) + \kappa I(t), \\ I'(t) = \chi E(t) - (\kappa + \delta + \zeta + \Gamma_1)I(t), \\ I_T'(t) = (1 - \chi)E(t) - (\zeta + \Gamma_2)I_T(t), \\ R'(t) = \delta I(t) - \zeta R(t), \end{cases} \quad (1)$$

With initial conditions $(S(0) = I_1, E(0) = I_2, I(0) = I_3, I_T(0) = I_4, R(0) = I_5)$.

The purpose of this research is to apply LSNN-GASQP to address the system of Equation (1). Table 1 provides the details on the parameters involved.

The remainder of the research is presented in the following manner: Section 2 outlines the proposed structure for the deterministic integrator LSNN-GASQP, while Section 3 highlights performance measurements; Section 4 discusses the results, and Section 5 concludes the study.

2. Methodology

The LSNN-GSQP system was designed to operate in two phases: utilizing LSNN frameworks and introducing an error-based fitness function. The necessary information was provided to execute a GA and SQP combination, maximizing the fitness value of the suggested technique.

2.1. Artificial neural network framework

This section describes the solution strategy for each class of the $SEIIR$ DM model. The mathematical equations are provided in relation to Equation (1), utilizing continuous LSNN mapping in accordance with the noted findings and the n^{th} order derivatives as follows in Equation (2):

$$\begin{cases} \ddot{S}(t) = \sum_{c=1}^b \alpha_{S,c} \Omega(\mu_{S,c}(t) + r_{S,c}) \\ \ddot{E}(t) = \sum_{c=1}^b \alpha_{E,c} \Omega(\mu_{E,c}(t) + r_{E,c}) \\ \ddot{I}(t) = \sum_{c=1}^b \alpha_{I,c} \Omega(\mu_{I,c}(t) + r_{I,c}) \\ \ddot{I}_T(t) = \sum_{c=1}^b \alpha_{I_T,c} \Omega(\mu_{I_T,c}(t) + r_{I_T,c}) \\ \ddot{R}(t) = \sum_{c=1}^b \alpha_{R,c} \Omega(\mu_{R,c}(t) + r_{R,c}) \\ \vdots \\ \ddot{S}^n(t) = \sum_{c=1}^b \alpha_{S,c} \Omega^n(\mu_{S,c}(t) + r_{S,c}) \\ \ddot{E}^n(t) = \sum_{c=1}^b \alpha_{E,c} \Omega^n(\mu_{E,c}(t) + r_{E,c}) \\ \ddot{I}^n(t) = \sum_{c=1}^b \alpha_{I,c} \Omega^n(\mu_{I,c}(t) + r_{I,c}) \\ \ddot{I}_T^n(t) = \sum_{c=1}^b \alpha_{I_T,c} \Omega^n(\mu_{I_T,c}(t) + r_{I_T,c}) \\ \ddot{R}^n(t) = \sum_{c=1}^b \alpha_{R,c} \Omega^n(\mu_{R,c}(t) + r_{R,c}) \end{cases} \quad (2)$$

Table 1. Explanation of the diabetes mellitus model's parameters

Variables	Interpretation	Values
ν	Population growth of the human species	1
ζ	Rate of natural death	0.00123
ψ	Contact frequency between susceptible and exposed groups	0.0009
ω	Frequency of contact between susceptible groups and those exposed to genetic effects	0.00005
κ	The rate of transmission from the infected population to the exposed population due to insulin use	0.0024
χ	The speed at which exposed people become infected people	0.004
δ	The illness rate of the infected population turned into a population that recovered due to insulin	0.3
Γ_1	Death rate without meditation	0.00139
Γ_2	Death rate due to insulin-receiving treatment	0.00134

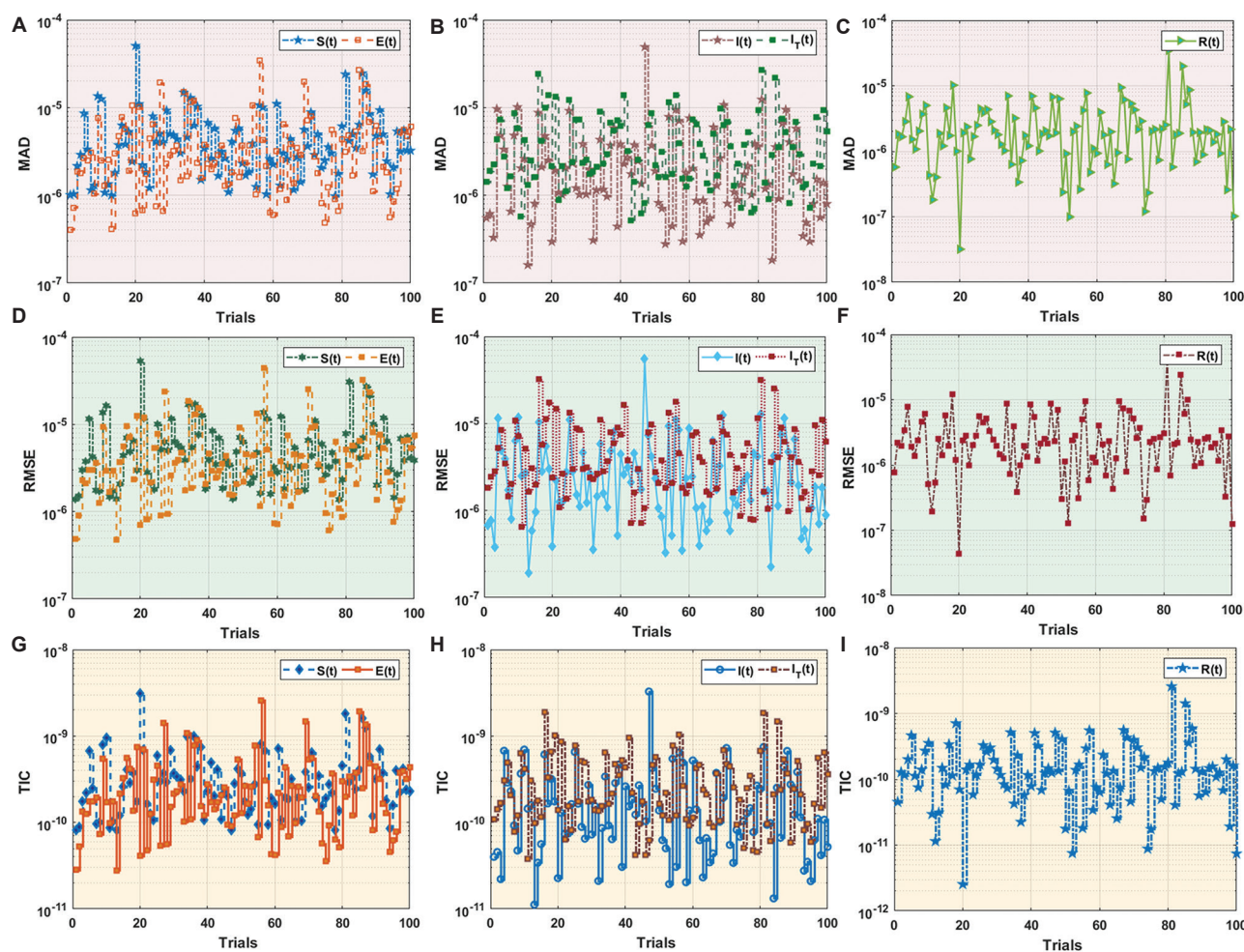


Figure 1. Analysis of convergence based on performance measurements of mean absolute deviation (MAD), root mean squared error (RMSE), and Theil's inequality coefficient (TIC) using the log-sigmoid neural network-genetic algorithm-based sequential quadratic programming for the diabetes mellitus model. Convergence analysis of MAD for the groups (A) $S(t)$ and $E(t)$, (B) $I(t)$ and $I_T(t)$, and (C) $R(t)$. Convergence analysis of RMSE for the groups (D) $S(t)$ and $E(t)$, (E) $I(t)$ and $I_T(t)$, and (F) $R(t)$. Convergence analysis of TIC for the groups (G) $S(t)$ and $E(t)$, (H) $I(t)$ and $I_T(t)$, and (I) $R(t)$. Abbreviations: E: Exposed; I: Infected without treatment; I_T : Infected with treatment; R: Recovered; S: Susceptible.

The activation function in the model, denoted by the notation Ω , and b determines the number of neurons in the network. W stands for the unknown (weights), written as Equation (3):

$$W = [W_S, W_E, W_I, W_{I_T}, W_R] \quad (3)$$

Where

$$W_S = [\alpha_S, \mu_S, r_S], W_E = [\alpha_E, \mu_E, r_E], W_I = [\alpha_I, \mu_I, r_I], \\ W_{I_T} = [\alpha_{I_T}, \mu_{I_T}, r_{I_T}], W_R = [\alpha_R, \mu_R, r_R]$$

and the components of weight are defined as follows in Equation (4):

$$\alpha_S = [\alpha_{S,1}, \alpha_{S,2}, \dots, \alpha_{S,b}], \mu_S = [\mu_{S,1}, \mu_{S,2}, \dots, \mu_{S,b}], r_S = [r_{S,1}, r_{S,2}, \dots, r_{S,b}]$$

$$\alpha_E = [\alpha_{E,1}, \alpha_{E,2}, \dots, \alpha_{E,b}], \mu_E = [\mu_{E,1}, \mu_{E,2}, \dots, \mu_{E,b}], r_E = [r_{E,1}, r_{E,2}, \dots, r_{E,b}] \\ \alpha_I = [\alpha_{I,1}, \alpha_{I,2}, \dots, \alpha_{I,b}], \mu_I = [\mu_{I,1}, \mu_{I,2}, \dots, \mu_{I,b}], r_I = [r_{I,1}, r_{I,2}, \dots, r_{I,b}] \\ \alpha_{I_T} = [\alpha_{I_T,1}, \alpha_{I_T,2}, \dots, \alpha_{I_T,b}], \mu_{I_T} = [\mu_{I_T,1}, \mu_{I_T,2}, \dots, \mu_{I_T,b}], \\ r_{I_T} = [r_{I_T,1}, r_{I_T,2}, \dots, r_{I_T,b}] \\ \alpha_R = [\alpha_{R,1}, \alpha_{R,2}, \dots, \alpha_{R,b}], \mu_R = [\mu_{R,1}, \mu_{R,2}, \dots, \mu_{R,b}], r_R = [r_{R,1}, r_{R,2}, \dots, r_{R,b}] \quad (4)$$

In the neural network approach, the activation function is the log-sigmoid function. The log-sigmoid function is defined mathematically as: $\Omega(t) = \frac{1}{e^{-t} + 1}$. The n^{th} derivative of Ω is also an activation function since Ω is an activation function. Thus, we have Equation (5):

$$\begin{aligned}
 \ddot{S}(t) &= \sum_{c=1}^b \frac{\alpha_{S,c}}{1+e^{-(\mu_{S,c}(t)+r_{S,c})}} \\
 \ddot{E}(t) &= \sum_{c=1}^b \frac{\alpha_{E,c}}{1+e^{-(\mu_{E,c}(t)+r_{E,c})}} \\
 \ddot{I}(t) &= \sum_{c=1}^b \frac{\alpha_{I,c}}{1+e^{-(\mu_{I,c}(t)+r_{I,c})}} \\
 \ddot{I}_T(t) &= \sum_{c=1}^b \frac{\alpha_{I_T,c}}{1+e^{-(\mu_{I_T,c}(t)+r_{I_T,c})}} \\
 \ddot{R}(t) &= \sum_{c=1}^b \frac{\alpha_{R,c}}{1+e^{-(\mu_{R,c}(t)+r_{R,c})}} \\
 &\vdots \\
 \ddot{S}^n(t) &= \sum_{c=1}^b \frac{\mu_{S,c} \alpha_{S,c} e^{-(\mu_{S,c}(t)+r_{S,c})}}{\left(1+e^{-(\mu_{S,c}(t)+r_{S,c})}\right)^2} \\
 \ddot{E}^n(t) &= \sum_{c=1}^b \frac{\mu_{E,c} \alpha_{E,c} e^{-(\mu_{E,c}(t)+r_{E,c})}}{\left(1+e^{-(\mu_{E,c}(t)+r_{E,c})}\right)^2} \\
 \ddot{I}^n(t) &= \sum_{c=1}^b \frac{\mu_{I,c} \alpha_{I,c} e^{-(\mu_{I,c}(t)+r_{I,c})}}{\left(1+e^{-(\mu_{I,c}(t)+r_{I,c})}\right)^2} \\
 \ddot{I}_T^n(t) &= \sum_{c=1}^b \frac{\mu_{I_T,c} \alpha_{I_T,c} e^{-(\mu_{I_T,c}(t)+r_{I_T,c})}}{\left(1+e^{-(\mu_{I_T,c}(t)+r_{I_T,c})}\right)^2} \\
 \ddot{R}^n(t) &= \sum_{c=1}^b \frac{\mu_{R,c} \alpha_{R,c} e^{-(\mu_{R,c}(t)+r_{R,c})}}{\left(1+e^{-(\mu_{R,c}(t)+r_{R,c})}\right)^2}
 \end{aligned} \quad (5)$$

The fitness function for the DM model (Equation [1]) in terms of mean square is as follows in Equations (6)–(12):

$$\ddot{e}_{DMM} = \ddot{e}_1 + \ddot{e}_2 + \ddot{e}_3 + \ddot{e}_4 + \ddot{e}_5 + \ddot{e}_6 \quad (6)$$

$$\ddot{e}_1 = \frac{1}{B} \sum_{b=1}^B \left(\ddot{S}_b - v + (\zeta + \psi \ddot{E}_b + \omega) \ddot{S}_b \right)^2 \quad (7)$$

$$\ddot{e}_2 = \frac{1}{B} \sum_{b=1}^B \left(\ddot{E}_b - (\psi \ddot{E}_b + \omega) \ddot{S}_b + (\zeta + 1) \ddot{E}_b - \kappa \ddot{I}_b \right)^2 \quad (8)$$

$$\ddot{e}_3 = \frac{1}{B} \sum_{b=1}^B \left(\ddot{I}_b - \chi \ddot{E}_b + (\kappa + \delta + \zeta + \Gamma_1) \ddot{I}_b \right)^2 \quad (9)$$

$$\ddot{e}_4 = \frac{1}{B} \sum_{b=1}^B \left(\ddot{I}_{T_b} - (1 - \chi) \ddot{E}_b + (\zeta + \Gamma_2) \ddot{I}_{T_b} \right)^2 \quad (10)$$

$$\ddot{e}_5 = \frac{1}{B} \sum_{b=1}^B \left(\ddot{R}_b - \delta \ddot{I}_b + \zeta \ddot{R}_b \right)^2 \quad (11)$$

$$\ddot{e}_6 = \frac{1}{5} \left[\left((\ddot{S})_0 - l_1 \right)^2 + \left((\ddot{E})_0 - l_2 \right)^2 + \left((\ddot{I})_0 - l_3 \right)^2 + \left((\ddot{I}_T)_0 - l_4 \right)^2 + \left((\ddot{R})_0 - l_5 \right)^2 \right] \quad (12)$$

Where

$Hb=1$, $\ddot{S} = \ddot{S}(t_b)$, $\ddot{E} = \ddot{E}(t_b)$, $\ddot{I} = \ddot{I}(t_b)$, $\ddot{I}_T = \ddot{I}_T(t_b)$, $\ddot{R} = \ddot{R}(t_b)$ and $t_b = hb$.

The error optimization process for all DM model classes is $\ddot{e}_1 + \ddot{e}_2 + \ddot{e}_3 + \ddot{e}_4 + \ddot{e}_5$ and \ddot{e}_6 . It is an error function dependent on the initial state. To achieve the highest network weights attainable, where $\ddot{e}_{DMM} \rightarrow 0$, and for every class, the approximate solution that coincides with the accurate solution is: $\{\dot{S}(t) \rightarrow S(t), \dot{E}(t) \rightarrow E(t), \dot{I}(t) \rightarrow I(t), \dot{I}_T(t) \rightarrow I_T(t), \dot{R}(t) \rightarrow R(t)\}$.

2.2. Learning process of GA-based sequential quadratic programming

A thorough explanation of GASQP's optimization of the error-based Equation (6) characterizing the DM model

Table 2. Statistical measurements for the susceptible and exposed groups

Time (years)	Susceptible group			Exposed group		
	Minimum	Median	Semi-interquartile range	Minimum	Median	Semi-interquartile range
0.0	7.73E-08	3.88E-07	5.54E-07	4.39E-09	2.31E-07	3.26E-07
0.1	1.45E-08	1.29E-06	1.56E-07	1.82E-09	2.00E-06	1.39E-06
0.2	2.03E-07	4.71E-06	2.79E-06	3.24E-08	5.10E-06	3.87E-06
0.3	5.08E-08	6.02E-06	4.22E-06	5.00E-08	3.54E-06	4.08E-06
0.4	1.36E-08	5.22E-06	4.11E-06	2.68E-08	2.48E-06	2.11E-06
0.5	2.10E-08	2.39E-06	2.20E-06	2.516E-08	9.59E-07	1.29E-06
0.6	2.29E-09	1.41E-06	1.83E-06	4.96E-08	2.47E-06	1.62E-06
0.7	2.38E-08	2.26E-06	2.12E-06	6.45E-09	1.82E-06	1.26E-06
0.8	5.11E-07	2.78E-06	1.55E-06	6.22E-08	1.84E-06	1.07E-06
0.9	4.70E-09	4.027E-06	2.40E-06	2.91E-08	3.57E-06	3.41E-06
1.0	1.36E-07	3.94E-06	2.01E-06	4.69E-08	2.27E-06	2.19E-06

Table 3. Statistical measurements for the infected groups with and without treatment

Time (years)	Infected group without treatment			Infected group with treatment		
	Minimum	Median	Semi-interquartile range	Minimum	Median	Semi-interquartile range
0.0	7.08E-11	1.88E-07	4.79E-07	5.88E-09	1.54E-07	2.90E-07
0.1	6.96E-09	7.46E-07	9.71E-07	1.21E-07	2.38E-06	1.36E-06
0.2	4.17E-09	1.04E-06	1.01E-06	1.32E-07	4.45E-06	4.11E-06
0.3	6.71E-08	1.62E-06	1.49E-06	3.68E-09	4.045E-06	3.97E-06
0.4	6.54E-08	2.16E-06	1.22E-06	1.01E-07	3.05E-06	3.13E-06
0.5	2.38E-08	2.73E-06	1.83E-06	9.14E-10	1.88E-06	2.10E-06
0.6	7.29E-08	2.17E-06	2.13E-06	9.45E-09	2.38E-06	2.17E-06
0.7	5.51E-10	1.40E-06	2.19E-06	3.79E-08	2.44E-06	1.62E-06
0.8	1.05E-08	8.08E-07	1.94E-06	3.44E-08	2.76E-06	2.34E-06
0.9	1.05E-08	1.317E-06	2.07E-06	1.61E-08	3.13E-06	3.31E-06
1.0	2.17E-10	7.70E-07	1.57E-06	9.06E-08	3.41E-06	3.02E-06

Table 4. Statistical measurements for the recovered group

Time (years)	Minimum	Median	Semi-interquartile range
0.0	1.426E-12	1.111E-08	1.408E-07
0.1	1.205E-08	1.619E-07	1.215E-07
0.2	1.044E-08	2.230E-06	1.487E-06
0.3	2.309E-08	2.100E-06	1.790E-06
0.4	4.500E-09	2.486E-06	1.851E-06
0.5	3.521E-08	2.315E-06	1.559E-06
0.6	5.104E-08	1.626E-06	1.183E-06
0.7	1.426E-08	1.114E-06	1.408E-06
0.8	1.205E-09	1.616E-06	1.215E-06
0.9	1.044E-08	2.232E-06	1.487E-06
1.0	2.307E-09	2.100E-06	1.795E-06

is given. GA is employed as an optimization technique. With the help of the best training strategy, GA is utilized to provide precise population results for solving rigid systems. To obtain the optimal system values in GA, selection, crossover, reproduction, and mutation were used. By combining SQP with local search methods, the performance of GAs is effectively improved. Examples that use GASQP include the COVID-19 model,³⁵ the tuberculosis model,³⁶ the Lassa fever model,³⁷ the mosquito model,³⁸ the Thomas-Fermi system,³⁴ and singular models.³⁹ The method was applied in the MATLAB program (version R2025b) using GASQP hybridization to determine the LSNN's unknown weight for the DM model in Equation (1).

3. Performance grades

The nonlinear DM model outlined in Equation (1) was computed using performance grades (mean absolute deviation

[MAD], root mean squared error [RMSE], Theil's inequality coefficient [TIC]). For related operations, the following algebraic formulas are provided in Equations (13)–(15):

$$\left\{ \begin{array}{l} MAD_S = \frac{1}{b} \sum_{c=1}^b \left| (S)_c - \left(\bar{S} \right)_c \right| \\ MAD_E = \frac{1}{b} \sum_{c=1}^b \left| (E)_c - \left(\bar{E} \right)_c \right| \\ MAD_I = \frac{1}{b} \sum_{c=1}^b \left| (I)_c - \left(\bar{I} \right)_c \right| \\ MAD_{I_T} = \frac{1}{b} \sum_{c=1}^b \left| (I_T)_c - \left(\bar{I}_T \right)_c \right| \\ MAD_R = \frac{1}{b} \sum_{c=1}^b \left| (R)_c - \left(\bar{R} \right)_c \right| \end{array} \right\} \quad (13)$$

$$\left\{ \begin{array}{l} RMSE_S = \sqrt{\frac{1}{b} \sum_{c=1}^b \left| \left((S)_c - \left(\bar{S} \right)_c \right)^2 \right|} \\ RMSE_E = \sqrt{\frac{1}{b} \sum_{c=1}^b \left| \left((E)_c - \left(\bar{E} \right)_c \right)^2 \right|} \\ RMSE_I = \sqrt{\frac{1}{b} \sum_{c=1}^b \left| \left((I)_c - \left(\bar{I} \right)_c \right)^2 \right|} \\ RMSE_{I_T} = \sqrt{\frac{1}{b} \sum_{c=1}^b \left| \left((I_T)_c - \left(\bar{I}_T \right)_c \right)^2 \right|} \\ RMSE_R = \sqrt{\frac{1}{b} \sum_{c=1}^b \left| \left((R)_c - \left(\bar{R} \right)_c \right)^2 \right|} \end{array} \right\} \quad (14)$$

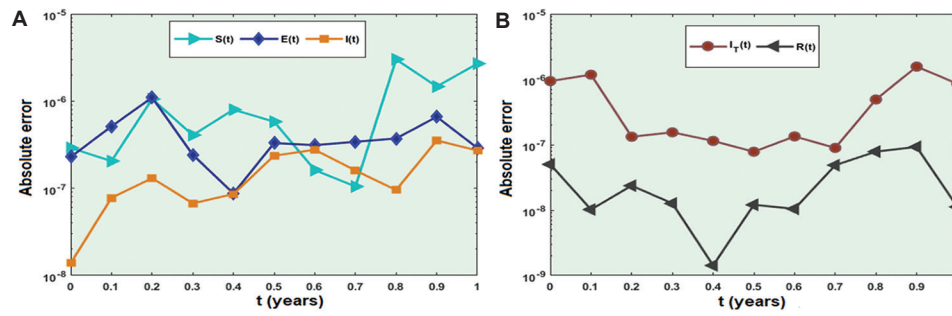


Figure 2. Absolute error for the diabetes mellitus model using log-sigmoid neural network-genetic algorithm-based sequential quadratic programming. (A) Absolute error for the groups $S(t)$, $E(t)$, and $I(t)$. (B) Absolute error for the groups $I_T(t)$ and $R(t)$. Abbreviations: E: Exposed; I: Infected without treatment; I_T: Infected with treatment; R: Recovered; S: Susceptible.

$$\left\{ \begin{array}{l} TIC_S = \frac{\sqrt{\frac{1}{b} \sum_{c=1}^b ((S)_c - (\ddot{S})_c)^2}}{\sqrt{\frac{1}{b} \sum_{c=1}^b (S)_c^2} + \sqrt{\frac{1}{b} \sum_{c=1}^b (\ddot{S})_c^2}} \\ TIC_E = \frac{\sqrt{\frac{1}{b} \sum_{c=1}^b ((E)_c - (\ddot{E})_c)^2}}{\sqrt{\frac{1}{b} \sum_{c=1}^b (E)_c^2} + \sqrt{\frac{1}{b} \sum_{c=1}^b (\ddot{E})_c^2}} \\ TIC_I = \frac{\sqrt{\frac{1}{b} \sum_{c=1}^b ((I)_c - (\ddot{I})_c)^2}}{\sqrt{\frac{1}{b} \sum_{c=1}^b (I)_c^2} + \sqrt{\frac{1}{b} \sum_{c=1}^b (\ddot{I})_c^2}} \\ TIC_{I_T} = \frac{\sqrt{\frac{1}{b} \sum_{c=1}^b ((I_T)_c - (\ddot{I}_T)_c)^2}}{\sqrt{\frac{1}{b} \sum_{c=1}^b (I_T)_c^2} + \sqrt{\frac{1}{b} \sum_{c=1}^b (\ddot{I}_T)_c^2}} \\ TIC_R = \frac{\sqrt{\frac{1}{b} \sum_{c=1}^b ((R)_c - (\ddot{R})_c)^2}}{\sqrt{\frac{1}{b} \sum_{c=1}^b (R)_c^2} + \sqrt{\frac{1}{b} \sum_{c=1}^b (\ddot{R})_c^2}} \end{array} \right. \quad (15)$$

$$\left\{ \begin{array}{l} S'(t) = 1 - (0.00123 + 0.0009E(t) + 0.00005)S(t) \\ E'(t) = (0.0009E(t) + 0.00005)S(t) - (0.00123 + 1) \\ E(t) + 0.0024I(t) \\ I'(t) = 0.004E(t) - \left(\begin{array}{l} 0.0024 + 0.3 + 0.00123 \\ + 0.00139 \end{array} \right) I(t) \\ I_T'(t) = (1 - 0.004)E(t) - (0.00123 + 0.00134)I_T(t) \\ R'(t) = 0.3I(t) - 0.00123R(t) \end{array} \right. \quad (16)$$

with initial conditions

$$\left\{ \begin{array}{l} S(0) = 0.27100271 \\ E(0) = 0.35682023 \\ I(0) = 0.00180668 \\ I_T(0) = 0.36133694 \\ R(0) = 0.00903342 \end{array} \right.$$

4. Results and discussion

This section provides a comprehensive review of the results obtained in the DM model solution (Equation [1]). A detailed examination using Adams' numerical outcomes validated the accuracy of the design using the LSNN-GASQP technique. Additionally, graphical and numerical statistics are presented to ensure the accuracy of the proposed technique. The nonlinear differential equation of the DM model (Equation [1]) has been adapted using the data from Table 2.

The fitness function based on error for the DM model (Equation [16]) is as follows in Equation (17):

$$\begin{aligned} \ddot{e}_{DMM} = & \frac{1}{B} \sum_{b=1}^B [(\ddot{S}_b - 1 + (0.00123 + 0.0009\ddot{E}_b \pm 0.00005)\ddot{S}_b)^2 + \\ & (\ddot{E}_b - (0.0009\ddot{E}_b + 0.00005)\ddot{S}_b + (0.00123 + 1)\ddot{E}_b - 0.0024\ddot{I}_b)^2 \\ & + (\ddot{I}_b - 0.004\ddot{E}_b + (0.0024 + 0.3 + 0.00123 + 0.00139)\ddot{I}_b)^2 \\ & + (\ddot{I}_{Tb} - (1 - 0.004)\ddot{E}_b + (0.00123 + 0.00134)\ddot{I}_{Tb})^2 \\ & + (\ddot{R}_b - 0.3\ddot{I}_b + 0.00123\ddot{R}_b)^2] + \frac{1}{5} [(\ddot{S}_0 - 0.27100271)^2 \\ & + (\ddot{E}_0 - 0.35682023)^2 + (\ddot{I}_0 - 0.00180668)^2 \\ & + (\ddot{I}_{T0} - 0.36133694)^2 + (\ddot{R}_0 - 0.00903342)^2] \end{aligned} \quad (17)$$

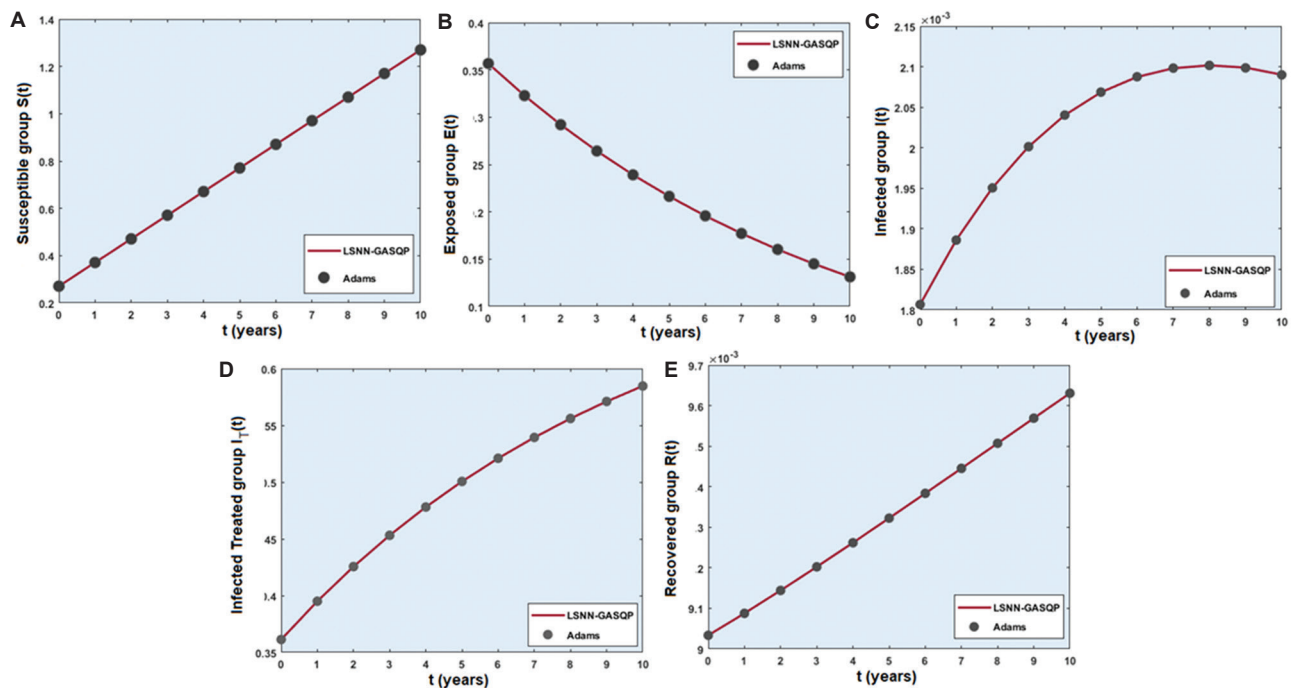


Figure 3. Comparison of the log-sigmoid neural network-genetic algorithm-based sequential quadratic programming (LSNN-GASQP) and the Adam numerical approach for the diabetes mellitus model. Comparison graphs for the groups (A) $S(t)$, (B) $E(t)$, (C) $I(t)$, (D) $I_T(t)$, and (E) $R(t)$. Abbreviations: E: Exposed; I: Infected without treatment; I_T: Infected with treatment; R: Recovered; S: Susceptible.

The developing LSNN-GASQP hybrid approach was employed in the DM model optimization process throughout a large number of trials to determine the appropriate weights for five neurons (100 iterations). Figure 1 illustrates the best LSNN weights. The acquired weight values were then entered into Equation (3), yielding an approximate solution in numerical representations, as shown in Equations (18)–(22):

$$S(t) = \frac{4.4329}{1 + e^{-(0.6971t + 1.7645)}} + \frac{3.9499}{1 + e^{-(0.3100t + 0.900)}} - \frac{4.9178814}{1 + e^{-(0.7374t + 2.356600)}} - \frac{3.201027}{1 + e^{-(0.7234t + 0.27561)}} - \frac{0.15267}{1 + e^{-(1.0353t - 2.601)}} \quad (18)$$

$$E(t) = \frac{-0.75336}{1 + e^{-(1.170748t + 0.9189)}} + \frac{0.6402}{1 + e^{-(0.30513t + 1.708)}} + \frac{0.4615}{1 + e^{-(0.17016t - 0.170)}} + \frac{1.164675}{1 + e^{-(0.817t - 2.597)}} + \frac{1.2997}{1 + e^{-(2.0774t - 3.00220)}} \quad (19)$$

$$I(t) = \frac{0.135}{1 + e^{-(0.069t - 0.990)}} - \frac{0.26787}{1 + e^{-(0.2290t + 0.581)}} + \frac{1.365}{1 + e^{-(0.4181t - 0.0043)}} + \frac{0.4505}{1 + e^{-(0.6079t - 1.262)}} - \frac{1.69511}{1 + e^{-(0.441671t - 0.483)}} \quad (20)$$

$$I_T(t) = \frac{0.2874}{1 + e^{-(1.26144t - 1.9138)}} - \frac{2.1238}{1 + e^{-(1.659t - 2.5013)}} + \frac{0.36199}{1 + e^{-(0.43032t - 1.9619)}} + \frac{0.71382}{1 + e^{-(0.80073t - 0.463)}} - \frac{0.1081}{1 + e^{-(0.15353t - 0.2088)}} \quad (21)$$

$$R(t) = \frac{0.58233}{1 + e^{-(0.11840t - 1.0358)}} - \frac{0.4198}{1 + e^{-(0.4401t - 0.2493)}} - \frac{0.063}{1 + e^{-(0.2593t - 0.07754)}} + \frac{0.189}{1 + e^{-(0.56570t - 0.2702)}} - \frac{0.0292}{1 + e^{-(0.1749060t - 0.52807)}} \quad (22)$$

Figure 2 illustrates the absolute error for each class of the DM model, comparing both techniques, which range from 10^{-9} to 10^{-5} . The comparison of the results of the GA-SQP and Adam numerical schemes is shown in Figure 3. Optimal weights for the DM model are shown in Figure 4, using LSNN-GASQP. A convergence analysis for the DM model using an LSNN-GASQP is presented in Figure 1, based on performance metrics including MAD, RMSE, and TIC. Figures 5–7 show the convergence assessment for the DM model using histograms of MAD, TIC, and RMSE, respectively. Figures 8–10 show the boxplots of MAD, RMSE, and TIC, respectively, using the LSNN-GASQP. Figure 1A–C shows the MAD performance metric for each class, which ranges from 10^{-8} to 10^{-4} . RMSE performance metrics for

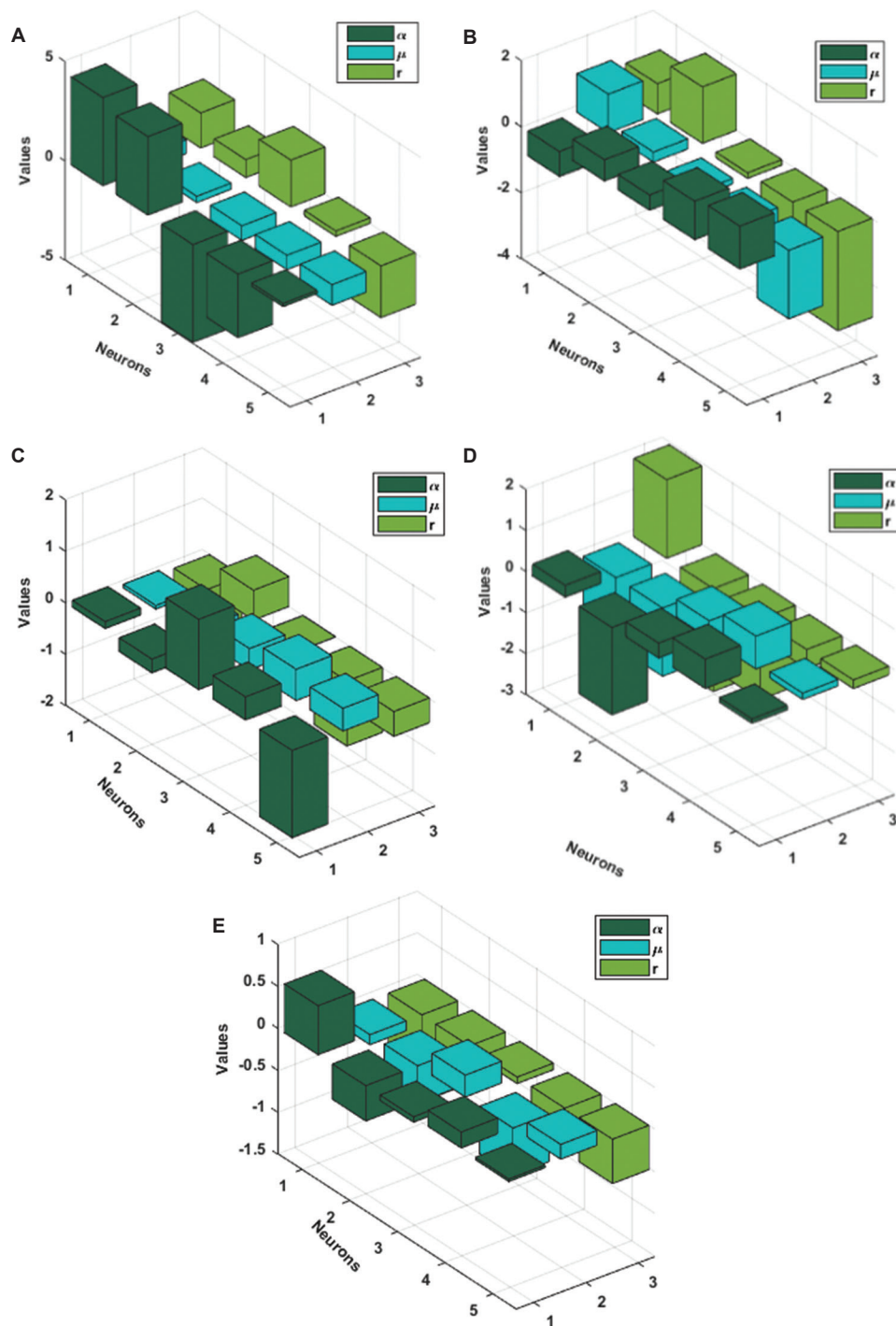


Figure 4. Optimal weights for the diabetes mellitus model using the log-sigmoid neural network-genetic algorithm-based sequential quadratic programming. Best weights for (A) $S(t)$, (B) $E(t)$, (C) $I(t)$, (D) $I_T(t)$, and (E) $R(t)$. Abbreviations: E: Exposed; I: Infected without treatment; I_T: Infected with treatment; R: Recovered; S: Susceptible.

each class are displayed in Figure 1D-F, with values ranging from 10^{-8} to 10^{-4} . TIC performance metrics for all classes, ranging from 10^{-12} to 10^{-8} , are shown in Figure 1G-I.

Figure 5 displays the MAD histogram values for all classes, ranging from 10^{-6} to 10^{-5} . Figure 6 displays the TIC histogram values for each class, which lie between 10^{-10}

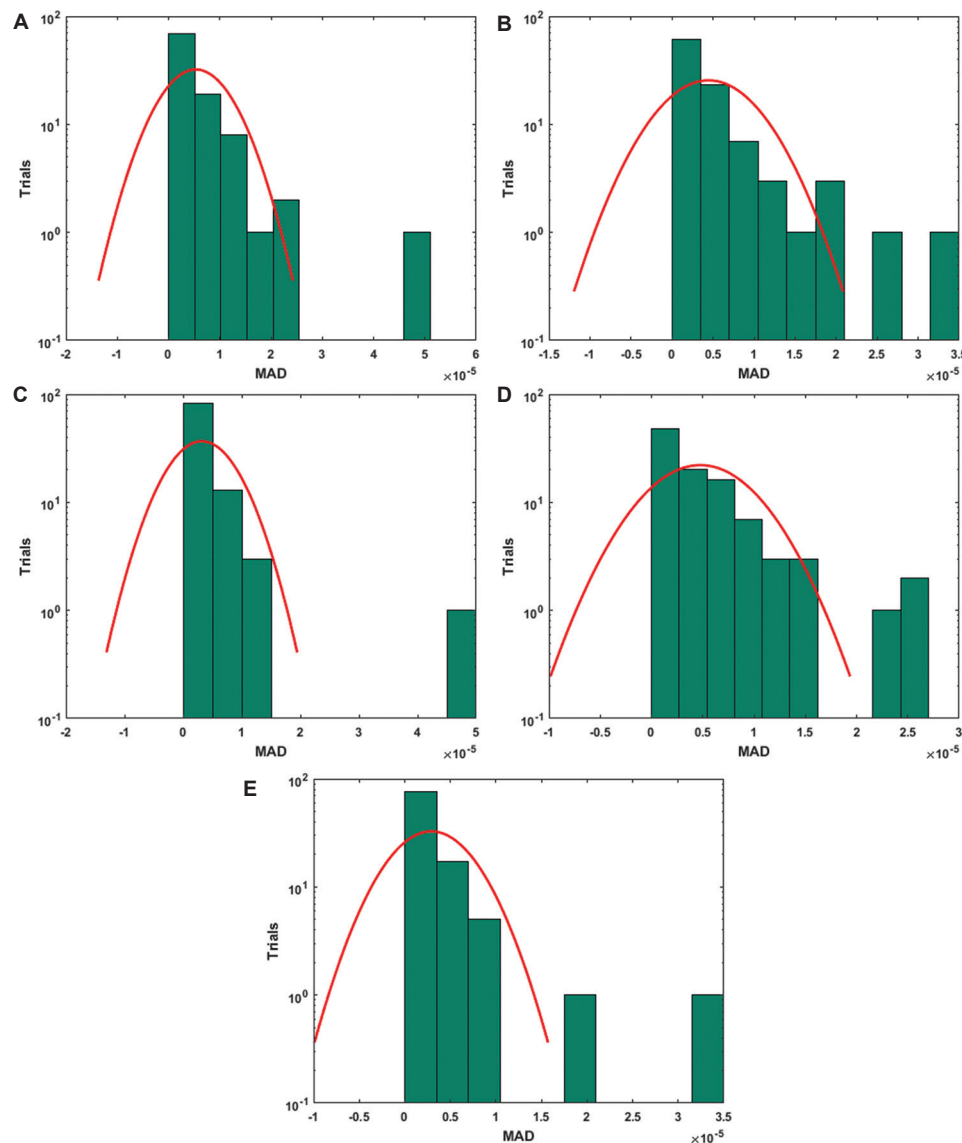


Figure 5. Convergence assessment for the diabetes mellitus model using histograms of mean absolute deviation (MAD). Histogram depiction of MAD for groups (A) $S(t)$, (B) $E(t)$, (C) $I(t)$, (D) $I_+(t)$, and (E) $R(t)$.

Abbreviations: E: Exposed; I: Infected without treatment; I_+ : Infected with treatment; R: Recovered; S: Susceptible.

and 10^{-9} . Figure 7 shows that the RMSE histogram values for each class fall within the range 10^{-6} to 10^{-5} . Figure 8 shows the MAD boxplot values for each class, ranging from 10^{-6} to 10^{-5} , while Figure 9 shows that the boxplot of RMSE values for all classes fall within the same range. The TIC boxplot values for each class are shown in Figure 10, with values ranging from 10^{-11} to 10^{-9} . The LSNN-GASQP solution was accurate and exact since all these statistical variables were very close to zero. To further validate the accuracy and precision of the LSNN-GASQP findings, statistical data analyses were performed using the semi-interquartile range (SIR), median (Med), and minimum

(Min) values. Tables 2-4 present statistics-based analysis of each class for the inputs between 0 and 1 with a step size of 0.1. These statistical results may not only demonstrate the numerical accuracy of the proposed framework but also prove its robustness and stability under various input scenarios. The near-zero error measure and minimal statistical spreads show that the technique performed consistently and reliably throughout multiple trials. This study demonstrates the hybrid LLNN-GASQP technique's generalization capacity and computational integrity, confirming its efficacy as a robust stochastic optimization framework for dealing with nonlinear dynamical systems.

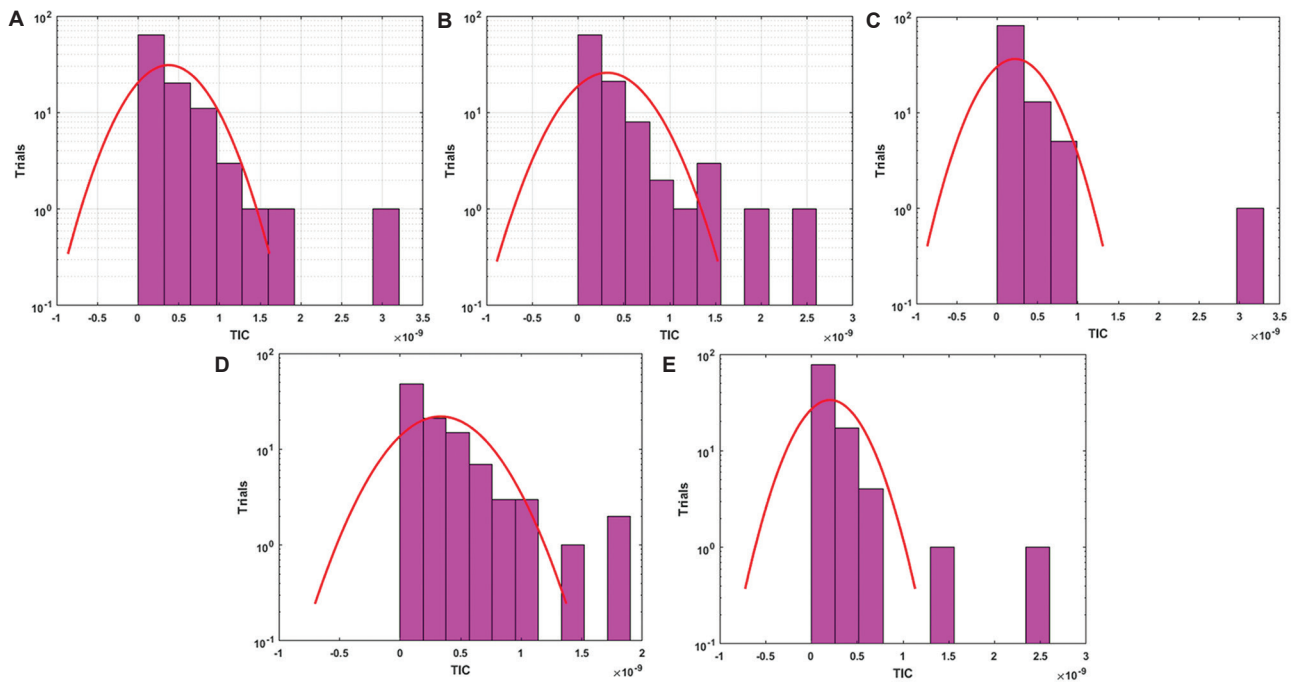


Figure 6. Convergence assessment for the diabetes mellitus model using histograms of Theil's inequality coefficient (TIC). Histogram depiction of TIC for groups (A) $S(t)$, (B) $E(t)$, (C) $I(t)$, (D) $I_T(t)$, and (E) $R(t)$.

Abbreviations: E: Exposed; I: Infected without treatment; I_T: Infected with treatment; R: Recovered; S: Susceptible.

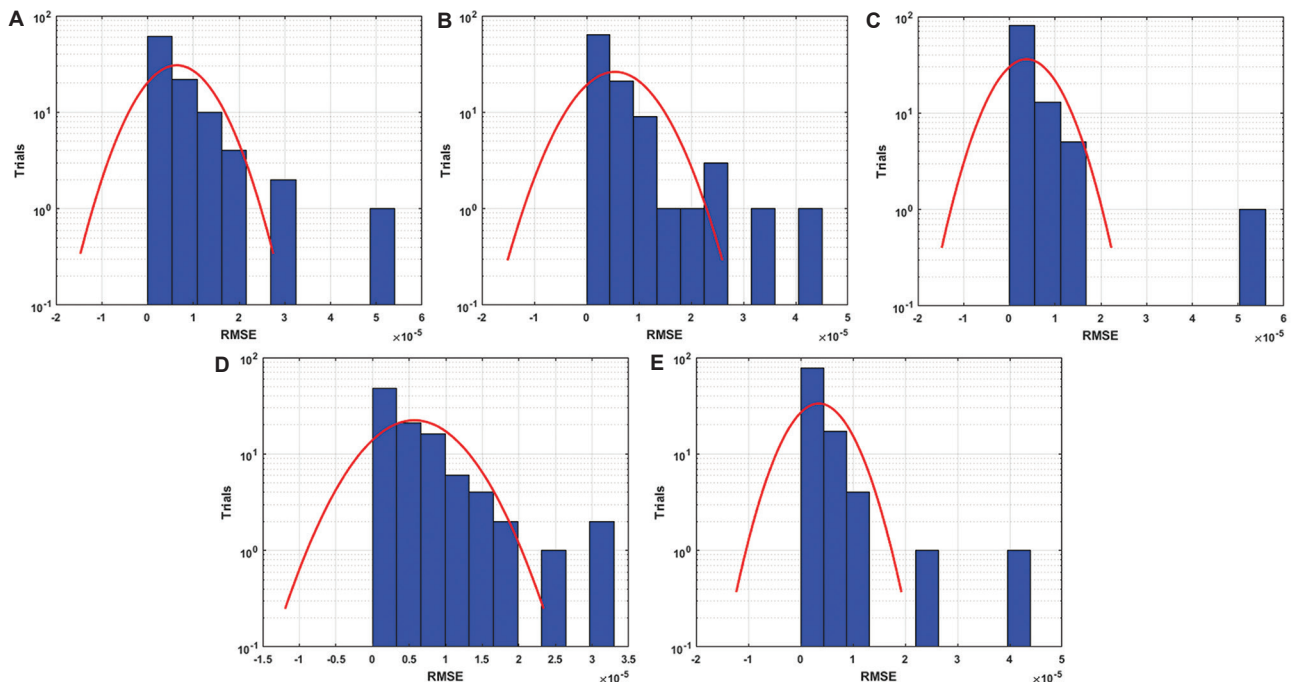


Figure 7. Convergence assessment for the diabetes mellitus model using histograms of root mean squared error (RMSE). Histogram depiction of RMSE for groups (A) $S(t)$, (B) $E(t)$, (C) $I(t)$, (D) $I_T(t)$, and (E) $R(t)$.

Abbreviations: E: Exposed; I: Infected without treatment; I_T: Infected with treatment; R: Recovered; S: Susceptible.

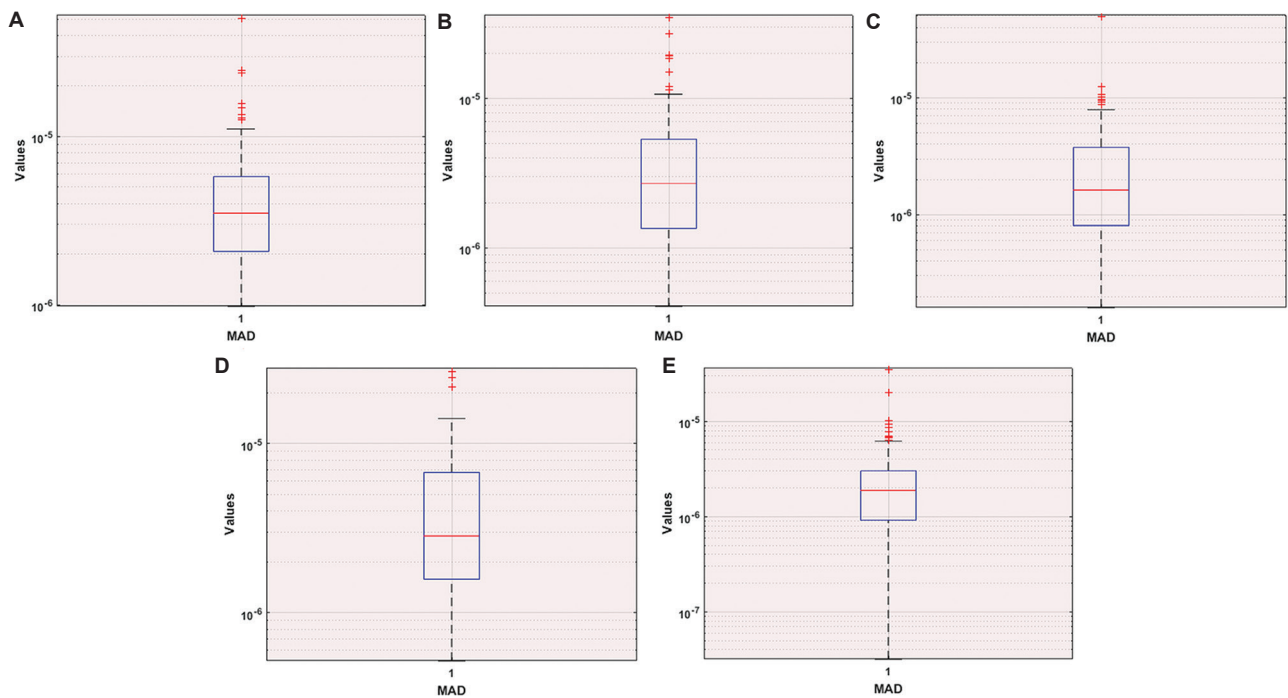


Figure 8. Convergence assessment for the diabetes mellitus model using boxplots depictions of performance metrics. Boxplot depiction of mean absolute deviation (MAD) for groups (A) $S(t)$, (B) $E(t)$, (C) $I(t)$, (D) $I_T(t)$, and (E) $R(t)$.

Abbreviations: E: Exposed; I: Infected without treatment; I_T: Infected with treatment; R: Recovered; S: Susceptible.

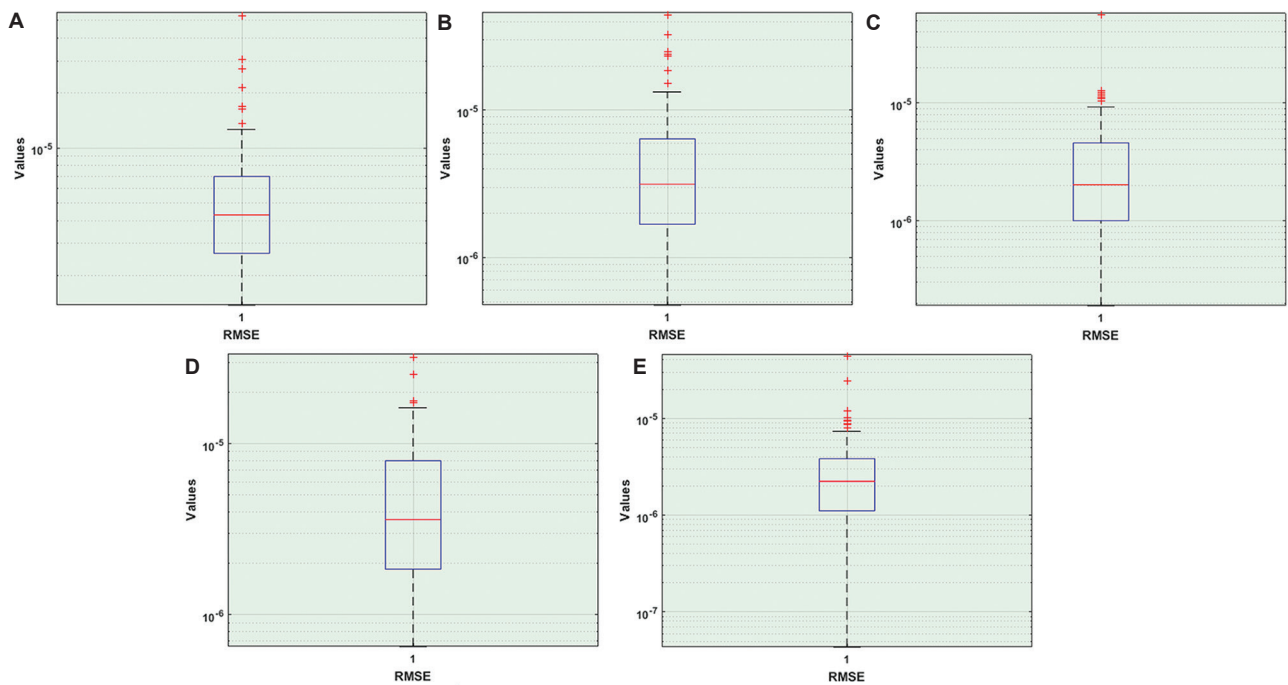


Figure 9. Convergence assessment for the diabetes mellitus model using boxplots depictions of root mean squared error (RMSE). Boxplot depiction of RMSE for groups (A) $S(t)$, (B) $E(t)$, (C) $I(t)$, (D) $I_T(t)$, and (E) $R(t)$.

Abbreviations: E: Exposed; I: Infected without treatment; I_T: Infected with treatment; R: Recovered; S: Susceptible.

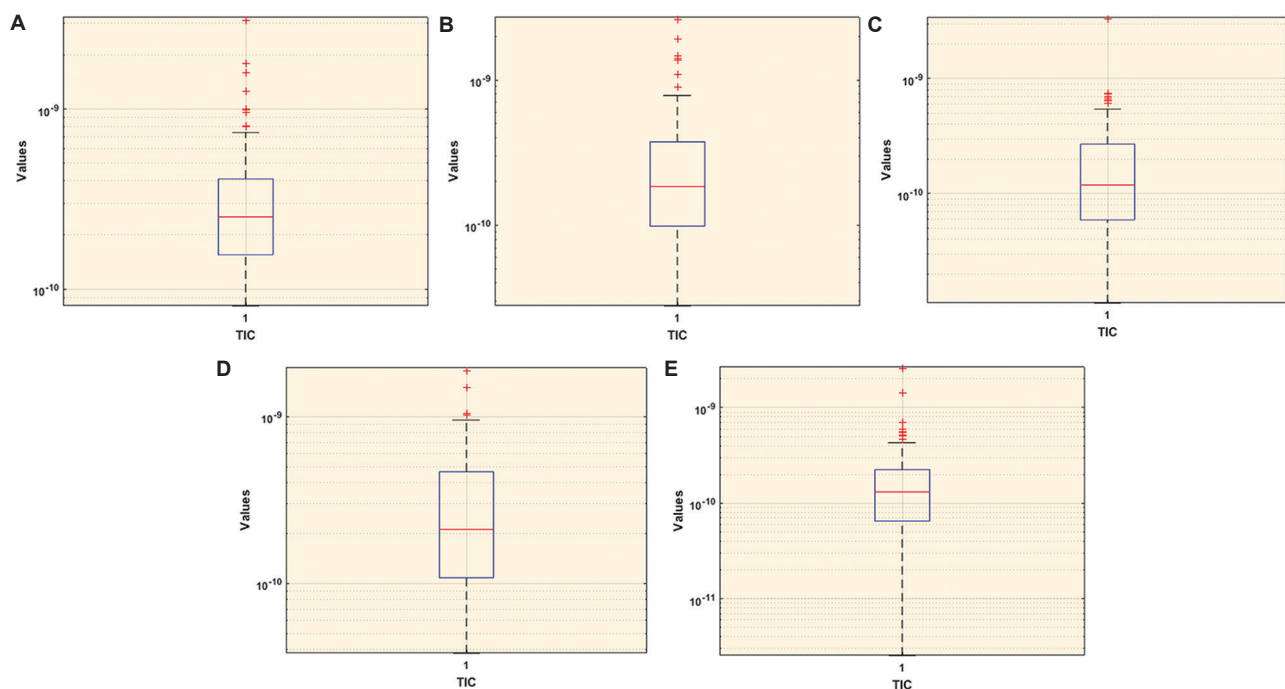


Figure 10. Convergence assessment for the diabetes mellitus model using boxplots depictions of Theil's inequality coefficient (TIC). Boxplot depiction of TIC for groups (A) $S(t)$, (B) $E(t)$, (C) $I(t)$, (D) $I_T(t)$, and (E) $R(t)$.

Abbreviations: E: Exposed; I: Infected without treatment; I_T: Infected with treatment; R: Recovered; S: Susceptible.

5. Conclusion

The novel computing hybrid LSNN-GASQP paradigm was used to solve the nonlinear DM model. SQP was used as a framework for local search, while the GA was used for global search. This prevented local minima and facilitated rapid convergence with great precision. This hybrid local optimizer utilizing a neural surrogate was an effective technique for calibrating nonlinear ordinary differential equations. The nonlinear differential equations DM model was used to construct a log-sigmoid fitness-based function, utilizing the mean squared error. The recommended paradigms' dependability, robustness, and efficacy were evaluated using the Adam numerical technique and absolute error analysis. The performance convergence criteria, calculated over 100 runs, comprised mean square error, generations, iterations, time, fitness evaluation, best global weight, and function counts, demonstrating how the suggested solution meets the rigorous specifications. The statistical analysis for 100 runs of the hybrid LSNN-GASQP used TIC, MAD, and RMSE. Their results illustrate the algorithm's precision to within 4 to 12 decimal places, indicating both numerical fidelity and durability rather than isolated success. Based on the Min, Med, and SIR operators, statistical indicators were employed to confirm the robustness of the suggested LSNN-GASQP. Min indicates the optimal-case

errors across the iterations, Med represents the standard error while mitigating outliers, and SIR illustrates the variability surrounding the median. The minimal values of Min, Med, and SIR summarized the performance of LSNN-GASQP, indicating good accuracy, consistency, and convergence.

Acknowledgments

None.

Funding

None.

Conflict of interest

The authors declare that they have no competing interests.

Author contributions

Conceptualization: Saba Kainat, Rashid Nawaz

Formal analysis: Rashid Nawaz, Saba Kainat

Investigation: All authors

Methodology: Saba Kainat, Muhammad Shoaib

Writing—original draft: Saba Kainat

Writing—review & editing: All authors

Ethics approval and consent to participate

Not applicable.

Consent for publication

Not applicable.

Availability of data

Not applicable.

References

1. Sastry K, Goldberg D, Kendall G. Genetic algorithms. In: Burke EK, Kendall G, editors. *Search Methodologies*. Boston, MA: Springer; 2005.
doi: 10.1007/0-387-28356-0_4
2. Das M, Roy A, Maity S, Kar S, Sengupta S. Solving fuzzy dynamic ship routing and scheduling problem through new genetic algorithm. *Decis Mak Appl Manag Eng*. 2022;5(2):329-361.
doi: 10.31181/dmame181221030d
3. Roy SK, De D. Genetic algorithm based internet of precision agricultural things (IopaT) for agriculture 4.0. *Int Things*. 2020;18:100201.
doi: 10.1016/j.iot.2020.100201
4. Squires M, Tao X, Elangovan S, Gururajan R, Zhou X, Acharya UR. A novel genetic algorithm based system for the scheduling of medical treatments. *Expert Syst Appl*. 2022;195:116464.
doi: 10.1016/j.eswa.2021.116464
5. Bozorgi Amiri A, Akbari M, Dadashpour I. A routing- allocation model for relief logistics with demand uncertainty: A genetic algorithm approach. *J Ind Eng Manag Stud*. 2022;8(2):93-110.
doi: 10.22116/jiems.2022.138125
6. Cassar DR, Santos GG, Zanotto ED. Designing optical glasses by machine learning coupled with a genetic algorithm. *Ceram Int*. 2021;47(8):10555-10564.
doi: 10.1016/j.ceramint.2020.12.167
7. Sang B. Application of genetic algorithm and BP neural network in supply chain finance under information sharing. *J Comput Appl Math*. 2021;384:113170.
doi: 10.1016/j.cam.2020.113170
8. Xu L, Hou L, Zhu Z, et al. Mid-term prediction of electrical energy consumption for crude oil pipelines using a hybrid algorithm of support vector machine and genetic algorithm. *Energy*. 2021;222:119955.
doi: 10.1016/j.energy.2021.119955
9. Berahas AS, Shi J, Yi Z, Zhou B. Accelerating stochastic sequential quadratic programming for equality constrained optimization using predictive variance reduction. *Comput Optim Appl*. 2023;86(1):79-116.
doi: 10.1007/s10589-023-00483-2
10. Xia L, Ling J, Xu Z, Bi R, Zhao W, Xiang S. Application of sequential quadratic programming based on active set method in cleaner production. *Clean Techn Environ Policy*. 2022;24(1):413-422.
doi: 10.1007/s10098-021-02207-8
11. Welhazi Y, Guesmi T, Alshammari BM, et al. A novel hybrid chaotic Jaya and sequential quadratic programming method for robust design of power system stabilizers and static VAR compensator. *Energies*. 2022;15(3):860.
doi: 10.3390/en15030860
12. Wang QJ. The genetic algorithm and its application to calibrating conceptual rainfall-runoff models. *Water Resour Res*. 1991;27(9):2467-2471.
doi: 10.1029/91WR01305
13. Mehmood A, Zameer A, Ling SH, Rehman AU, Raja MA. Integrated computational intelligent paradigm for nonlinear electric circuit models using neural networks, genetic algorithms and sequential quadratic programming. *Neural Comput Appl*. 2020;32(14):10337-10357.
doi: 10.1007/s00521-019-04573-3
14. Ilyas H, Ahmad I, Raja MA, Shoaib M. A novel design of Gaussian WaveNets for rotational hybrid nanofluidic flow over a stretching sheet involving thermal radiation. *Int Commun Heat Mass Transf*. 2021;123:105196.
doi: 10.1016/j.icheatmasstransfer.2021.105196
15. Sabir Z, Raja MA, Wahab HA, Shoaib M, Aguilar JF. Integrated neuro-evolution heuristic with sequential quadratic programming for second-order prediction differential models. *Numer Methods Partial Differ Equ*. 2024;40(1):e22692.
doi: 10.1002/num.22692
16. Du YT, Rayner CK, Jones KL, Talley NJ, Horowitz M. Gastrointestinal symptoms in diabetes: Prevalence, assessment, pathogenesis, and management. *Diabetes Care*. 2018;41(3):627-637.
doi: 10.2337/dc17-1536
17. Bayani MA, Shakiba N, Bijani A, Moudi S. Depression and quality of life in patients with type 2 diabetes mellitus. *Caspian J Intern Med*. 2022;13(2):335-342.
doi: 10.22088/cjim.13.2.3
18. Alzaman N, Ali A. Obesity and diabetes mellitus in the Arab world. *J Taibah Univ Med Sci*. 2016;11(4):301-309.
doi: 10.1016/j.jtumed.2016.03.009
19. Tummanapalli SS, Wang LL, Dhanapalaratnam R, et al. Moderate-severe peripheral neuropathy in diabetes associated with an increased risk of dry eye disease. *Optom Vis Sci*. 2024;101(9):563-570.
doi: 10.1097/OPX.0000000000002178
20. Abdulrahman D, Elkhoully S, Nematalla EH, Mostafa A.

- Effect of control of diabetes mellitus on corneal morphology. *Egypt J Ophthalmol.* 2022;2(2):86-98.
doi: 10.21608/ejomos.2022.110391.1044
21. Allen A, Iqbal Z, Green-Saxena A, *et al.* Prediction of diabetic kidney disease with machine learning algorithms, upon the initial diagnosis of type 2 diabetes mellitus. *BMJ Open Diabetes Res Care.* 2022;10(1):e002560.
doi: 10.1136/bmjdr-2021-002560
22. Marín-Peñalver JJ, Martín-Timón I, Sevillano-Collantes C, Del Cañizo-Gómez FJ. Update on the treatment of type 2 diabetes mellitus. *World J Diabetes.* 2016;7(17):354-395.
doi: 10.4239/wjd.v7.i17.354
23. De Vries JJ, Hoppenbrouwers T, Martinez-Torres C, *et al.* Effects of diabetes mellitus on fibrin clot structure and mechanics in a model of acute neutrophil extracellular traps (NETs) formation. *Int J Mol Sci.* 2020;21(19):7107.
doi: 10.3390/ijms21197107
24. Hajdu M, Knutsen MO, Vértés V, *et al.* Quality of glycemic control has significant impact on myocardial mechanics in type 1 diabetes mellitus. *Sci Rep.* 2022;12(1):20180.
doi: 10.1038/s41598-022-24619-2
25. Climie RE, Van Sloten TT, Bruno RM, *et al.* Macrovasculature and microvasculature at the crossroads between type 2 diabetes mellitus and hypertension. *Hypertension.* 2019;73(6):1138-1149.
doi: 10.1161/hypertensionaha.118.11769
26. Sabir Z, Raja MA, Baleanu D, Cengiz K, Shoaib M. Design of Gudermannian Neuroswarming to solve the singular Emden-Fowler nonlinear model numerically. *Nonlinear Dyn.* 2021;106(4):3199-3214.
doi: 10.1007/s11071-021-06901-6
27. Ali S, Ahmad I, Raja MA, Ahmad SU, Shoaib M. Design of evolutionary cubic spline intelligent solver for nonlinear Painlevé-I transcendent. *Int J Mod Phys B.* 2021;35(29):2150299.
doi: 10.1142/S0217979221502994
28. Umar M, Sabir Z, Raja MA, Aguilar JG, Amin F, Shoaib M. Neuro-swarm intelligent computing paradigm for nonlinear HIV infection model with CD4+ T-cells. *Math Comp Simul.* 2021;188:241-253.
doi: 10.1016/j.matcom.2021.04.008
29. Cui Q, Xu C, Ou W, *et al.* Further study on Hopf bifurcation and hybrid control strategy in BAM neural networks concerning time delay. *AIMS Math.* 2024;9(5):13265-13290.
doi: 10.3934/math.2024647
30. Ilyas H, Raja MA, Ahmad I, Shoaib M. A novel design of Gaussian wavelet neural networks for nonlinear Falkner-Skan systems in fluid dynamics. *Chin J Phys.* 2021;72:386-402.
doi: 10.1016/j.cjph.2021.05.012
31. Raja MAZ, Shah FH, Tariq M, Ahmad I, Ahmad SU. Design of artificial neural network models optimized with sequential quadratic programming to study the dynamics of nonlinear Troesch's problem arising in plasma physics. *Neural Comput Appl.* 2018;29(6):83-109.
doi: 10.1007/s00521-016-2530-2
32. Ahmad I, Raja MA, Ramos H, Bilal M, Shoaib M. Integrated neuro-evolution-based computing solver for dynamics of nonlinear corneal shape model numerically. *Neural Comput Appl.* 2021;33(11):5753-5769.
doi: 10.1007/s00521-020-05355-y
33. Fajri N, Sanusi, Asmaidi. SEIITR model for diabetes mellitus distribution in case of insulin and care factors. *J Inotera.* 2020;5(2):100-106.
doi: 10.31572/inotera.Vol5.Iss2.2020.ID113
34. Ahmad SU, Faisal F, Shoaib M, Raja MA. A new heuristic computational solver for nonlinear singular Thomas-Fermi system using evolutionary optimized cubic splines. *Eur Phys J Plus.* 2020;135(1):55.
doi: 10.1140/epjp/s13360-019-00066-3
35. Shoaib M, Abukhaled M, Kainat S, Nisar KS, Raja MA, Zubair G. Integrated neuro-evolution-based computing paradigm to study the COVID-19 transposition and severity in Romania and Pakistan. *Int J Comput Intell Syst.* 2022;15(1):80.
doi: 10.1007/s44196-022-00133-1
36. Shoaib M, Kainat S, Raja MA, Nisar KS. Design of artificial neural networks optimized through genetic algorithms and sequential quadratic programming for tuberculosis model. *Waves Random Complex Media.* 2025;35(5):8243-8266.
doi: 10.1080/17455030.2022.2094028
37. Shoaib M, Tabassum R, Raja MA, Nisar KS, Alqahtani MS, Abbas M. A design of predictive computational network for transmission model of Lassa fever in Nigeria. *Results Phys.* 2022;39:105713.
doi: 10.1016/j.rinp.2022.105713
38. Umar M, Raja MA, Sabir Z, Alwabri AS, Shoaib M. A stochastic computational intelligent solver for numerical treatment of mosquito dispersal model in a heterogeneous environment. *Eur Phys J Plus.* 2020;135(7):565.
doi: 10.1140/epjp/s13360-020-00557-8
39. Sabir Z, Wahab HA. Evolutionary heuristic with Gudermannian neural networks for the nonlinear singular models of third kind. *Phys Scr.* 2021;96(12):125261.
doi: 10.1088/1402-4896/ac3c56